HIGH-GRADIENT TESTING OF SINGLE-CELL TEST CAVITIES AT KEK / NEXTEF

Tetsuo Abe*, Yoshio Arakida, Toshiyasu Higo, Shuji Matsumoto, and Toshikazu Takatomi
High Energy Accelerator Research Organization (KEK), Tsukuba, Japan
Xiowei Wu[1] and Jiaru Shi[1]
Department of Engineering Physics, Tsinghua University, Beijing, China
[1]also at Key Laboratory of Particle & Radiation Imaging, Ministry of Education, Beijing, China

Abstract

So far, we have developed X-band high-gradient accelerating structures of prototypes for normal-conducting linear colliers in a comprehensive way, establishing a full production process including fabrication and test. On the other hand, focusing on the fact that we do not know both the high-gradient limit of performance and breakdown trigger mechanism on the normal-conducting RF acceleration, we have built a new test stand for fresh basic study on RF breakdown in vacuum, where we use compact test structures with an RF field concentrated in a single test cell.

In this paper, we report on the status of the new test stand called "Nextef / Shield-B," including its trigger system and various detectors installed to Shield-B.

INTRODUCTION

X-band normal-conducting RF acceleration technology can be applied to high-gradient accelerators, such as compact linear colliders and medical linacs. Based on the development results and experiences obtained through the NLC/GLC projects [1] (aiming at an operational gradient of 65 MV/m), high-gradient accelerating structures with higher-order-mode (HOM) damped structure (hereinafter simply referred to as damped structure) have been developed, aiming at an operational gradient of 100 MV/m [2]. Through this development, we have been establishing a full production process including fabrication and test of multi-cell prototype structures.

One of the recent significant achievements is a high-gradient test result of a prototype structure for CLIC [3], which meets requirements from the CLIC design: an accelerating gradient of 100 MV/m, an RF pulse width around 200 ns, a repetition rate of 50 Hz, and a breakdown rate (BDR) lower than 3×10^{-7} /m/pulse although such structure has no damped structure (i.e. undamped structure) [4]. The final design of the CLIC accelerating structure has a heavily damped structure with HOM waveguides (waveguide damped structure), and recent prototype structures based on such design were high-gradient tested, and found to have approximately two orders of magnitude higher BDR than that of the corresponding undamped ones [5]. Although it has been found that such large BDR difference is related to large surface currents due to opening of the HOM waveguides [6, 7], we do not yet fully understand the real reason, and in addition, we do not know the real cause of breakdown (breakdown trigger mechanism); these two facts have motivated us to perform further basic study on breakdown characteristics of the structures.

In parallel with the above-mentioned comprehensive development of multi-cell prototypes, we have built a new test stand focused on basic study on RF breakdown in vacuum based on the collaboration among the high-gradient accelerating-structure development teams at CERN, SLAC, Tsinghua University, and KEK. Here, we use compact test cavities with an RF field concentrated in a single test cell coupled with both an upstream coupling cell and a downstream end cell. This is a minimum structure keeping a realistic RF field for acceleration in the test cell; we refer to this three-cavity structure as "single-cell structure." This high-gradient testing method, originating from [8], is more time-saving and cost-effective compared with such comprehensive development because such single-cell cavities are easy to make and test.

In this paper, we describe the experimental setup, including the trigger system and various detectors installed to Shield-B, together with examples of data acquired with the detectors. Finally, we show the current status and the future plan.

OVERVIEW OF THE TEST STAND

Figure 1 shows the X-band (11.4 GHz) test facility: Nextef, which consists of two radiation shields called Shield-A and Shield-B, where we use PPM klystrons originally developed for the GLC project. In Shield-A, we perform high-gradient tests of multi-cell prototypes, while in Shield-B, high-gradient tests for basic study using single-cell structures have started.

Experimental Setup

Figure 2 shows the experimental setup in Shield-B. We have installed two sets of directional couplers located upstream of the mode converter (TE_{10} mode in the rectangular waveguide (WR90) to TM_{01} mode in the circular waveguide (WC90)), one of which is used to measure RF power, the other to monitor RF waveforms using RF detectors with a time constant shorter than 10 ns, for both input and reflected waves. A pickup antenna is attached to the vacuum duct downstream of the test cavity. Along the beam line[1], we

* tetsuo.abe@kek.jp

[1] Note that we use the word "beam line" for convenience; no beam is injected into test cavities during high-gradient tests.

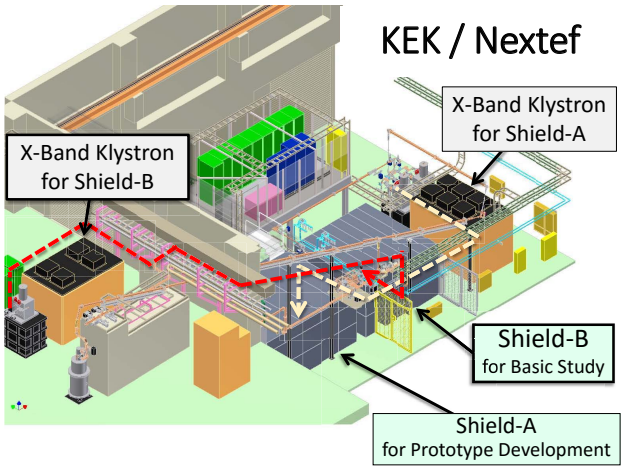

Figure 1: X-band test facility: Nextef. The red (light yellow) dashed line indicates a power line for Shield-B (Shield-A).

have installed Faraday cups, an X-ray detector, and a TV camera.

Figure 3 shows the currently-tested cavity with choke-mode damped structure [9].

Electromagnetic Field

Figure 4 shows an excited electromagnetic field in the test cavity during high-gradient testing, which is a π-mode of the three-cavity system with TM_{010} mode in each cell. It should be emphasized that any test cavity is designed so that an excited field is a standing wave with the highest field in the central test cell. Typically, peak electric field in the test cell is approximately twice of that in other two cells (coupling and end cells), as shown in Fig. 4(a).

RF Pulse Shaping

In order to have a constant high field in the test cell as long as possible, we shape the RF pulse into two steps as shown in Fig. 5(a). In the first step for 100 ns, we charge RF energy in the test cavity ("charging step"). At the end of the charging step, we suddenly decrease the RF power down to approximately one third of that in the charging step so that we maintain constant RF field in the second step for 100 to 300 ns ("maintaining step"), as shown in Fig. 5(b). Because test cavities are designed to have an input matching, the reflection in the maintaining step should be small.

Trigger System

Breakdown candidate events are triggered by setting a threshold for currents measured with the Faraday cups. In addition, we have introduced waveform of the reflected wave in this system (see the next section for details). If such current exceeds a specified threshold, or the waveform of the reflected wave differs significantly from the normal one, the output from the klystron is stopped, and the data acquisition (DAQ) system collects and stores all related data.

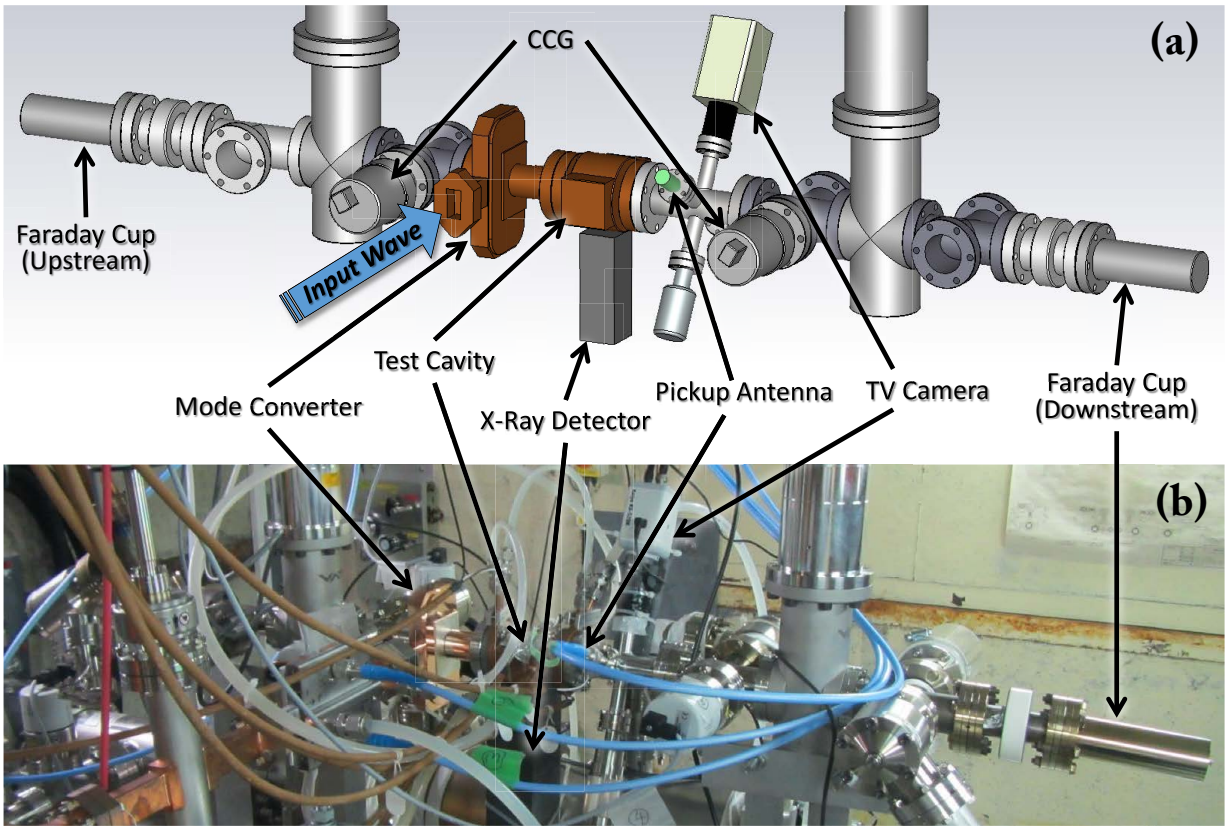

Figure 2: Experimental setup for high-gradient tests in Shield-B. (a) Schematic diagram. (b) Photograph of the actual setup as of July 29, 2016.

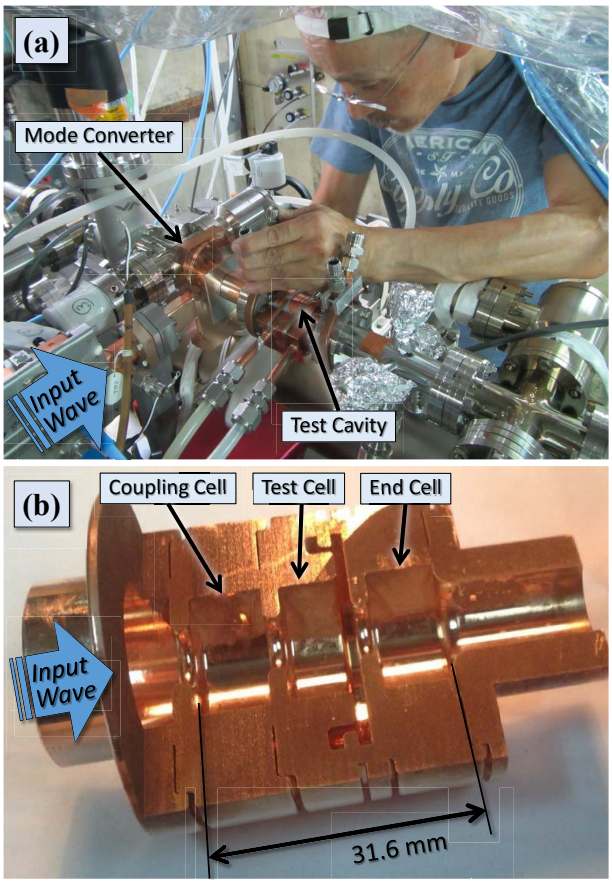

Figure 3: Current status in Shield-B. (a) Installation of the test cavity to Shield-B on July 7, 2016. (b) Prototype of the test cavity, cut in halves for inspection.

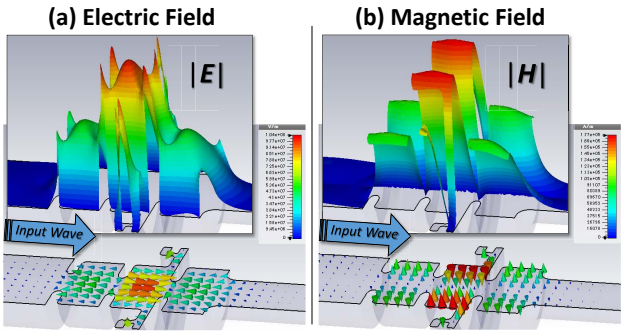

Figure 4: Electromagnetic field excited in the test cavity, simulated for an input RF power of 1 MW by using CST MICROWAVE STUDIO / frequency-domain solver. Top two figures show magnitude of the field as a height of the carpet in linear scale.

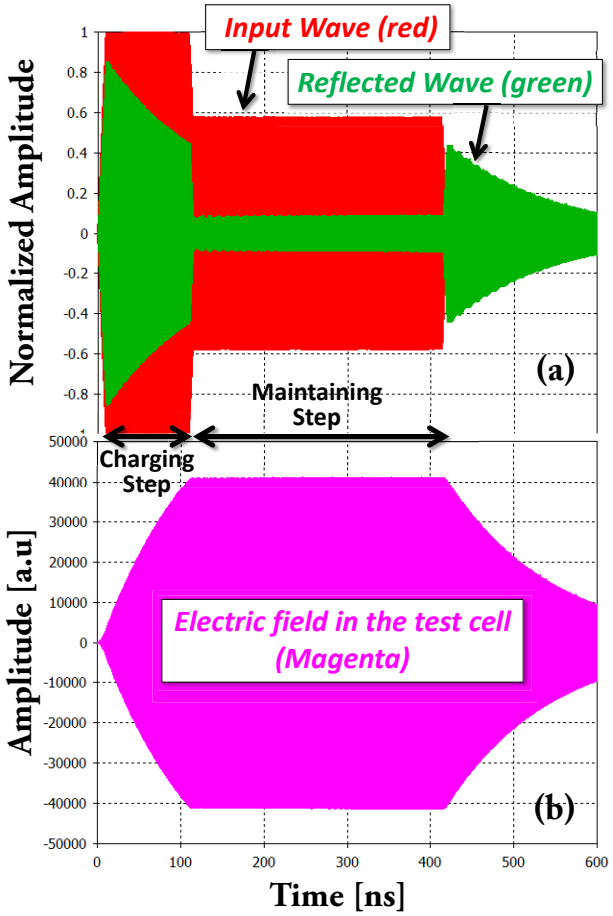

Figure 5: Time-domain simulation using CST MICROWAVE STUDIO for a monochromatic input wave of 11.4 GHz. (a) Input and reflected waves, both of which are normalized so that the amplitude of the input wave in the charging step is one. (b) Electric field excited in the test cell for the input wave in (a).

BREAKDOWN-RELATED SIGNALS

In the following subsections, we explain breakdown-related signals acquired with the detectors installed to Shield-B.

RF Waveforms

Figure 6 shows trigger logics using reflection waveforms ("reflection waveform trigger") together with examples of related data. We have developed the reflection waveform trigger, consisting of the following three logics:

- "Overall threshold": if the highest reflection level exceeds a specified threshold, the event is triggered. In the case that breakdown occurs in the charging step, as shown in Fig. 6(b), the event can be triggered by this logic. However, in the case that breakdown occurs in the maintaining step, this logic is ineffective because the RF power in the maintaining step is significantly

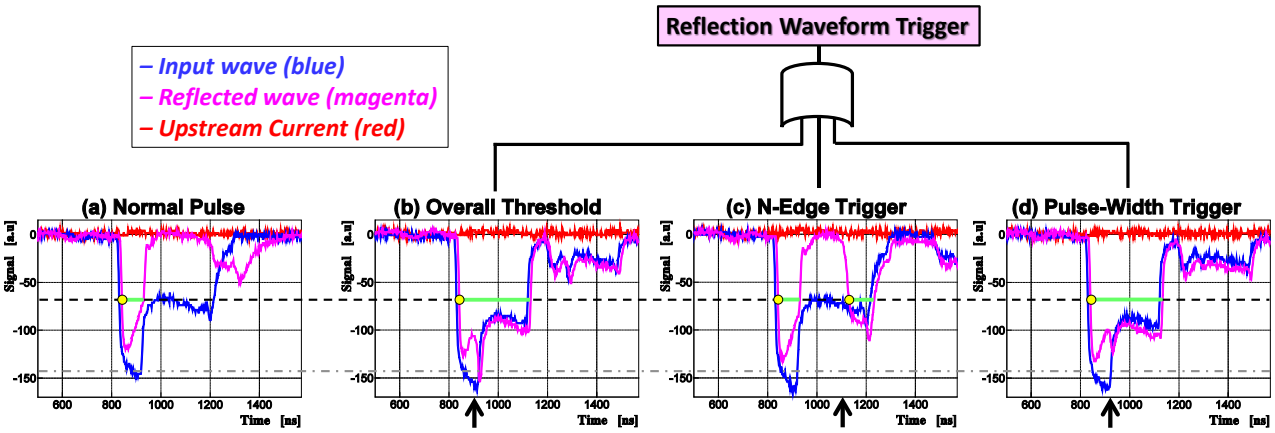

Figure 6: Examples of experimental waveform data (input RF power ≈ 1.3 MW, gradient ≈ 57 MV/m) which can be acquired with this trigger system. Gray dashed-dotted line (black dashed line) indicates an example of the overall threshold (trigger level for the N-edge and pulse-width trigger logics). Yellow circles indicate edge of the falling slope at the trigger level. Green lines indicate pulse width between edges of the falling and rising slopes at the trigger level. Arrows indicate estimated timing when breakdown occurred. (a) Example of normal RF pulses. (b)-(d) Example of breakdown candidate events which can be triggered by the overall threshold, N-edge trigger logic, or pulse-width trigger logic, respectively.

lower than that in the charging step, so that the reflection level at breakdown timing is lower than that in the charging step, as seen in Fig. 6(c).

- "N-edge": if number of edges of the falling slope at a specified trigger level exceeds one within an RF-pulse repetition period, as shown in Fig. 6(c), the event is triggered. This logic is effective in the case that breakdown occurs within the maintaining step. However, if breakdown occurs during the transient period from the charging to maintaining step, this logic might be ineffective because reflection-level rise might be merged to the reflection wave in the charging step as seen in Fig. 6(d).
- "Pulse-width": if pulse width between edges of the falling and rising slopes at a specified trigger level is outside a specified range (an example of the specified range: [50, 110] ns), as shown in Fig. 6(d), the event is triggered. This is effective even in the case that breakdown occurs during such transient period (e.g. Fig. 6(d)).

Here highest reflection level, number of the edges, and pulse widths are fast detected, and the output from the klystron is stopped within 10 μs of breakdown. Usually, events triggered by the overall threshold can be also triggered by the pulse-width trigger logic, so that the N-edge and pulse-width trigger logics are essential, and these two logics form a complete waveform trigger system.

Current Flash

During high-gradient testing, there are dark currents originated from field-emitted electrons. However, such current is under the noise level in this test, as seen in Fig. 6(a). When breakdown occurs, we often observe large instantaneous current ("current flash") although its detailed mechanism is unknown. Figure 7 shows an example of current-flash

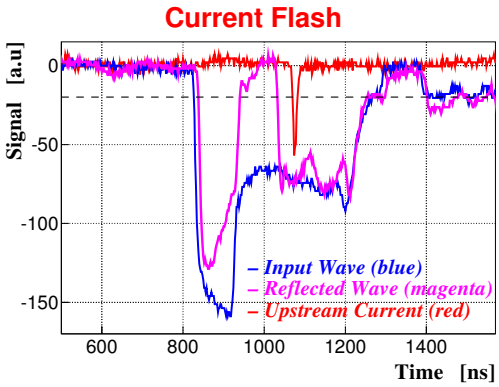

Figure 7: Example of current-flash events (input RF power ≈ 1.3 MW, gradient ≈ 57 MV/m). The threshold of the current-flash trigger is shown with a dashed line.

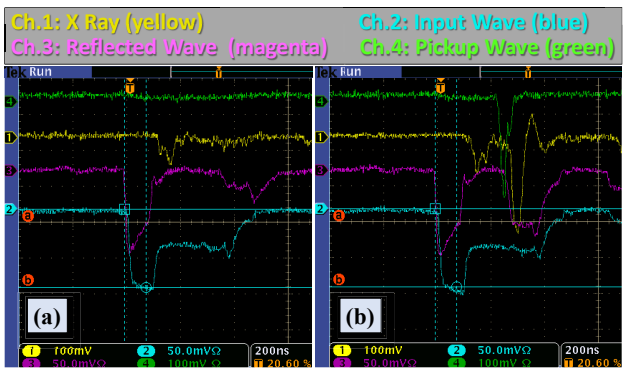

Figure 8: Example of X-ray signals (input RF power ≈ 1.3 MW, gradient ≈ 57 MV/m). (a) Normal RF pulse. (b) Breakdown candidate event acquired by the current-flash trigger.

events. A clear spike was observed in the current signal, and this event was acquired by the current-flash trigger. It should be noted that such type of current flash does not always accompany with breakdown; e.g. the breakdown candidate events shown in Figs. 6(b)-(d) had no current flash.

X Ray

X rays are generated when field-emitted electrons accelerate and impact inner surfaces of the cavity. We have installed an X-ray detector, consisting of scintillator and photomultiplier, located under the test cavity, as shown in Fig. 2. Figure 8(b) shows an example of X-ray signals, where a much larger spike than in the normal RF pulse in Fig. 8(a) was observed in the breakdown candidate event.

Video Image of the Cavity

Direct observation of inside of test cavities should be helpful information [10]. We have installed a TV camera and a mirror, as shown in Fig. 9(a). Figure 9(b) shows an example of TV video images for a breakdown candidate event. So far, we have observed various types of significant discharges in many breakdown candidate events, however, in not all of the breakdown candidate events.

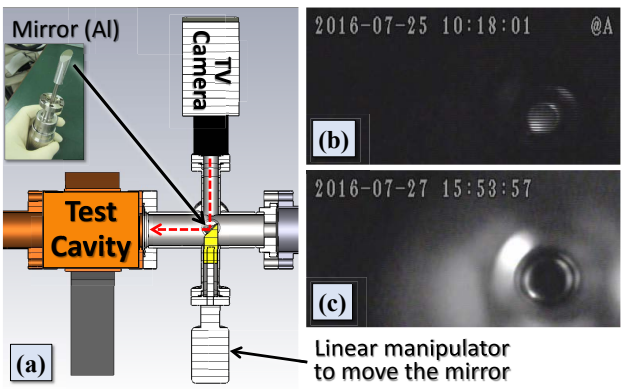

Figure 9: (a) Setup of the TV camera and mirror. (b) Example of acquired TV video images with discharge observed at the moment of trigger timing for a breakdown candidate event. (c) TV video image when we turned the RF switch off, and injected a light to the cavity through one of the view ports (for comparison).

STATUS AND PLAN

We have started the experimental basic study at Nextef / Shield-B with the various detectors, where the DAQ and trigger systems are operating smoothly. BDR measurements and correlation study among the data acquired by the various detectors have been performed for the first series of test cavities with the choke-mode damped structure. After the first series, we will perform a high-gradient test for the quadrant-type single-cell test cavity [11], which is an interesting and promising structure, followed by CLIC-type waveguide damped structures.

ACKNOWLEDGMENTS

We greatly appreciate the support from the CLIC team in financial and technical aspects. This is endorsed by the agreement between CERN and KEK (ICA-JP-0103).

We also thank Dr. V. Dolgashev and Prof. S. Tantawi of SLAC for valuable discussions. This collaboration is supported by the US-Japan Cooperative Program in High Energy Physics.

Finally, we are grateful to the members of KEK e^+e^- Injector Linac for their support of the Nextef operation.

REFERENCES

[1] J. Wang and T. Higo, "Accelerator Structure Development for NLC/GLC," ICFA Beam Dynamics Newsletter **32**, 27, 2003.

[2] T. Higo *et al.*, "High Gradient Performance of TW Accelerator Structures Targeting 100 MV/m," in Proceedings of the 12th Annual Meeting of Particle Accelerator Society of Japan, August 2015 (Paper ID: WEP047).

[3] M. Aicheler *et al.*, "A Multi-TeV Linear Collider Based on CLIC Technology : CLIC Conceptual Design Report," CERN-2012-007, SLAC-R-985, KEK-Report-2012-1, PSI-12-01, JAI-2012-001.

[4] T. Higo *et al.*, "Advancement of High Gradient Study at 100 MV/m Range," in Proceedings of the 8th Annual Meeting of Particle Accelerator Society of Japan, August 2011 (Paper ID: TUPS129).

[5] T. Higo *et al.*, "Comparison of High Gradient Performance in Varying Cavity Geometries," in Proceedings of IPAC2013, Shanghai, China, 2013 (Paper ID: WEPFI018).

[6] V. Dolgashev, S. Tantawi, Y. Higashi, and B. Spataro, "Geometric dependence of radio-frequency breakdown in normal conducting accelerating structures," Applied Physics Letters 97, 171501 (2010).

[7] F. Wang, C. Adolphsen and C. Nantista, "Performance limiting effects in X-band accelerators," Phys. Rev. ST Accel. Beams **14**, 010401 (2011) Addendum: [Phys. Rev. ST Accel. Beams **15**, 120402 (2012)]. doi:10.1103/PhysRevSTAB.15.120402, 10.1103/PhysRevSTAB.14.010401.

[8] V. A. Dolgashev, S. G. Tantawi, C. D. Nantista, Y. Higashi and T. Higo, "Travelling Wave and Standing Wave Single Cell High Gradient Tests," SLAC-PUB-10667, 2004.

[9] X. Wu, T. Abe, H. Chen, T. Higo, J. Shi, W. Wuensch and H. Zha, "High Power Test of X-band Single Cell HOM-free Choke-mode Damped Accelerating Structure made by Tsinghua University," doi:10.18429/JACoW-IPAC2016-THPOR043, 2016.

[10] T. Abe *et al.*, "Breakdown study based on the direct in-situ observation of inner surfaces of an RF accelerating cavity during a high-gradient test," Phys. Rev. Accel. Beams **19**, 102001 (2016).

[11] T. Abe *et al.*, "Fabrication of Quadrant-Type X-Band Single-Cell Structure used for High Gradient Tests," in Proceedings of the 11th Annual Meeting of Particle Accelerator Society of Japan, August 2014 (Paper ID: SUP042).